J. Fluid Mech. (1972), *vol.* 55, *part* 2, *pp.* 289–300
Printed in Great Britain

A note on the angular dispersion of a fluid line element in isotropic turbulence

By S. CORRSIN AND M. J. KARWEIT
Mechanics Department, The Johns Hopkins University

(Received 31 January 1972)

The mean-square angular displacement of a fluid material line element is expressed as an integral of the corresponding angular velocity in material coordinates, with forms like those in Taylor's (1921) linear displacement analysis. Measurements using a hydrogen-bubble tracer in isotropic turbulence show that the mean-square angular velocity of a line is of the same order of magnitude as the mean-square vorticity, and that its 'Lagrangian' integral time scale is of the order of the inverse of the r.m.s. vorticity. The angular velocity of a line element is also formulated in spatial co-ordinates. Finally, the connexion between angular dispersion and the approach toward isotropy is pointed out.

1. Introduction

The statistical problem of turbulent dispersion of a fluid material point from a designated location was first formulated in a natural way by Taylor (1921), by relating the mean-square displacement to the autocorrelation function of the point velocity represented in material ('Lagrangian') co-ordinates. Much of the research on this problem since that time, including the generalization to pairs of points, has been summarized by Batchelor & Townsend (1956), by Lumley (1962) and by Corrsin (1962). Little work seems to have been done directly upon the *angular dispersion* of an infinitesimal fluid material line (to be called a 'line element') under similar circumstances. It is our purpose to report a first simple look at this question.

2. Representation in material co-ordinates

Consider a line element represented in a 'right-handed' Cartesian co-ordinate system. We are interested in the evolution of the statistical properties of the unit vector **l**, whose components are the direction cosines. However, the actual angular dispersion is in a sense more naturally tied to the behaviour of angles such as $\theta_{(1)}, \theta_{(2)}$ and $\theta_{(3)}$, those given by projection on the Cartesian planes (see figure 1). In particular, if we ever take an interest in statistically isotropic orientation, this will be most easily stated as the constancy of the probability density functions of the angles, as observed,† over 2π.

† This is not the same as the actual total angles because the appearance of the line element is the same for $\theta_{(i)} = \alpha, \alpha+\pi, \alpha+2\pi$, etc. If the two ends of the element can be distinguished (like the feather end and the business end of an arrow), then the appearance is the same for $\theta_{(i)} = \alpha, \alpha+2\pi, \alpha+4\pi, \ldots$.

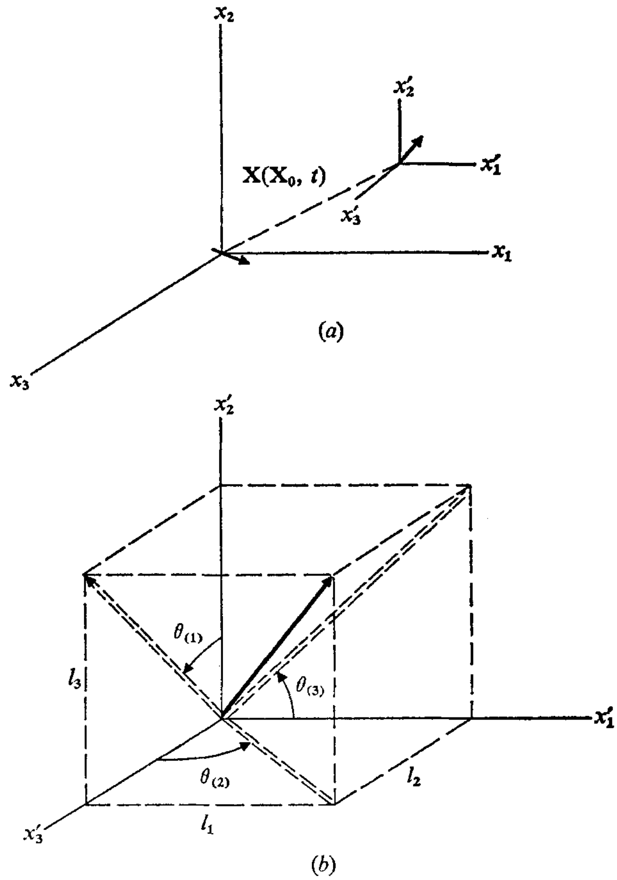

FIGURE 1. Notation for the line element. (a) The initial position at $t = t_0$ and the position at $t = t$. (b) Direction cosines and projected angles.

The angles $\theta_{(i)}$ made by the line element can be written in material co-ordinates $\mathbf{a}$ as $\Theta_{(i)}(\mathbf{a}, t)$, where $\mathbf{a}$ identifies the fluid material point. The corresponding observed angular velocity is

$$B_{(i)} \equiv \partial\Theta_{(i)}(\mathbf{a}, t)/\partial t. \tag{1}$$

The subscript on $\Theta_{(i)}$ is bracketed to remind us that this is not a Cartesian component of a vector.

Equation (1) can be 'integrated with respect to t' (actually we integrate the equation of its characteristics) to give

$$\Theta_{(i)}(\mathbf{a}, t) = \Theta_{(i)}(\mathbf{a}, t_0) + \int_{t_0}^{t} B_{(i)}(\mathbf{a}, t)\, dt_1, \tag{2}$$

which is analogous to Taylor's representation of a displacement component. For simplicity, we put the x_1 axis along the direction of the element at $t = t_0$. Then

$$\Theta_{(1)}(\mathbf{a}, t_0) = 0, \quad \Theta_{(2)}(\mathbf{a}, t_0) = \Theta_{(3)}(\mathbf{a}, t_0) = \tfrac{1}{2}\pi. \tag{3}$$

Multiplying (2) for $i = 1$ by $B_{(1)}(\mathbf{a}, t)$, then forming the ensemble average, we get what might be called the 'angular diffusivity':

$$\frac{1}{2}\frac{d}{dt}\overline{\Theta^2_{(1)}} = \int_{t_0}^{t} \overline{B_{(1)}(\mathbf{a}, t)\, B_{(1)}(\mathbf{a}, t_1)}\, dt_1. \tag{4}$$

For further simplicity, we restrict the turbulence to being isotropic and statistically stationary (a physically contradictory pair of conditions, of course, but useful for some purposes), so that

$$\overline{B_{(i)}(\mathbf{a}, t)\, B_{(i)}(\mathbf{a}, t \pm \tau)} = L(\tau). \tag{5}$$

Then (4) can be written as

$$\frac{1}{2}\frac{d}{dt}\overline{\Theta^2_{(1)}} = \int_{0}^{t-t_0} L(\tau)\, d\tau. \tag{6}$$

Integrating again yields

$$\overline{\Theta^2_{(1)}}(t) = 2\int_{0}^{t-t_0}\int_{0}^{t^*} L(\tau)\, d\tau\, dt^*, \tag{7}$$

and integrating this by parts gives a single-integral form, viz.

$$\overline{\Theta^2_{(1)}}(t) = 2\int_{0}^{t-t_0} (t - t_0 - \tau)\, L(\tau)\, d\tau. \tag{8}$$

Asymptotic behaviour for $t \to t_0$ and for $t - t_0 \to \infty$ can also be written in forms analogous to those in Taylor's displacement analysis. As $B_{(i)}$ is a stationary random function of t, $L(\tau)$ is even, so its Maclaurin series is

$$L(\tau) = L(0) + L''(0)\frac{\tau^2}{2!} + L^{\text{iv}}(0)\frac{\tau^4}{4!} + \dots \tag{9}$$

or, in terms of $B_{(i)}$ itself,

$$L(\tau) = \overline{B^2_{(i)}} - \overline{\left[\frac{\partial B_{(i)}}{\partial t}\right]^2}\frac{\tau^2}{2!} + \dots. \tag{10}$$

By introducing the symbol $N(\tau) \equiv L(\tau)/L(0)$ for the correlation function, and

$$\lambda_B \equiv \left[\frac{1}{2\overline{B^2}}\overline{\left(\frac{\partial B}{\partial t}\right)^2}\right]^{-\frac{1}{2}} = \left[\frac{L''(0)}{2L(0)}\right]^{-\frac{1}{2}} \tag{11†}$$

for the abscissa intercept of the vertex-osculating parabola of $N(\tau)$, we can rewrite (10) as

$$N(\tau) = 1 - \tau^2/\lambda_B^2 + \dots. \tag{12}$$

The small-time behaviour of the mean-square angular displacement is then given by (7) or (8) as

$$\overline{\Theta^2_{(1)}} \to \overline{B^2}(t - t_0)^2\{1 - (t - t_0)^2/6\lambda_B^2\}. \tag{13}$$

The corresponding behaviour for $t - t_0 \to \infty$ follows from (8) under the assumptions that the necessary integrals are finite constants for $t - t_0 = \infty$:

$$\overline{\Theta^2_{(1)}} \to 2\overline{B^2}\left\{(t - t_0)\int_{0}^{t-t_0} N(\tau)\, d\tau - \int_{0}^{t-t_0} \tau N(\tau)\, d\tau\right\}_{(t-t_0)\to\infty}, \tag{14}$$

† From this point on we omit the subscript on B for simplicity.

or
$$\overline{\Theta^2_{(1)}} \to 2\overline{B^2}\{T_B(t-t_0) - S_B\}_{(t-t_0)\to\infty}, \tag{15}$$
where
$$T_B \equiv \int_0^\infty N(\tau)\,d\tau$$
is the integral time scale of the angular velocity. If it is assumed that the large τ behaviour of $N(\tau)$ is such that S_B, the second integral in (14), 'reaches' its asymptotic value for finite large $(t-t_0)$,† the first term in (15) will eventually dominate, and (15) simplifies to the classical 'Brownian motion' form associated with gas molecules,
$$\overline{\Theta^2_{(1)}} \to 2\overline{B^2}T_B(t-t_0), \tag{16}$$
which corresponds to constant 'angular diffusivity':
$$\mathscr{D}_\Theta \to \overline{B^2}T_B. \tag{17}$$

Clearly it would be interesting to relate the mean-square angular velocity $\overline{B^2}$ and the two time scales λ_B and T_B to better known properties in terms of either material ('Lagrangian') or spatial ('Eulerian') co-ordinates.

3. An experiment

Hydrogen-bubble lines perpendicular to the mean flow have been photographed in nearly isotropic, grid-generated turbulence in a water tunnel (Corrsin & Karweit 1969). The grid Reynolds number based on the mesh size (0·5 in.) and empty tunnel mean speed (4·0 in./s) was 1360, a 'small' value, which gave a turbulence Reynolds number based on Taylor microscale and r.m.s. turbulent component velocity of $R_\lambda \approx 5$.

As each marked fluid line drifted downstream from the electrolysis wire (located at $x_{01}/M = 18$, i.e. 18 mesh lengths behind the grid), it became increasingly convoluted. At each of seven downstream distances, the randomly convoluted line was sampled at ten positions equally spaced across the tunnel section. The corresponding readings of $\theta_{(3)}(x_1 - x_{01})$ taken from 36 lines at each station were plotted to give empirical probability density functions (actually 'frequency functions') $f_\Theta(\gamma; \Delta x_1/M)$. Here $\Delta x_1 \equiv x_1 - x_{01}$ and M is grid mesh size. At each station the ten sample positions were far enough apart for the $\theta_{(3}$ readings to be essentially independent, so each frequency function was described by 360 independent data points.

We are interested in samples uniformly spaced, or randomly spaced without bias, along the fluid contour itself. With respect to that objective, our measured density functions $f_\Theta(\gamma; \Delta x_1/M)$ were biased in favour of line regions with $|\theta_{(3)}| \ll 1$, so they had to be 'corrected'. The desired density function is related to the measured one in principle by
$$p_\Theta(\gamma; \Delta x_1/M) = f_\Theta(\gamma; \Delta x_1/M)/|\cos\gamma|. \tag{18}$$

† For the mathematical reader, it should be noted that the (weaker) necessary and sufficient condition for this asymptotic form is that $L(\tau)$ be 'Césaro-1 integrable' to a non-zero value (Lumley 1970).

$\frac{\Delta x_1}{M} = \frac{\bar{U}\Delta t}{M}$	$\bar{U}\Delta s/M$ (see equation (30))	$\overline{\Theta^2_{(3)}}$ (rad)^2	$(\overline{\Theta^2_{(3)}})^{\frac{1}{2}}$ (rad)
2·44	1·98	0·0912	0·302
4·88	4·16	0·252	0·503
7·32	5·60	0·50	0·707
9·76	7·24	0·765	0·875
12·20	8·85	0·812	0·901
14·64	9·94	0·835	0·915
17·08	11·20	1·22	1·106

TABLE 1

Because of the singularity this is inconvenient, so we actually used $\theta_{(3)}$ values at intervals of 10°, and the approximate 'correction'

$$p_\Theta(\gamma; \Delta x_1/M) \approx f_\Theta(\gamma; \Delta x_1/M) \Big/ \frac{1}{10}\int_{\gamma-5^\circ}^{\gamma+5^\circ} |\cos\gamma_1|\, d\gamma_1. \tag{19}$$

From the resulting collection of probability density functions the 'measured' mean-square angular displacements were computed (table 1). In order to relate these data to the stationary turbulence analysis of the previous section, they must be 'corrected' for the effects of downstream decay.

4. 'Correction' for decay

A fairly detailed discussion of velocity covariance rescaling has been given by, among others, Comte-Bellot & Corrsin (1971).† Here we use analogous procedures for the rescaling of angular velocity. The objective can be stated as follows: we have a non-stationary random variable $B(t)$ and want to rescale both B and t to generate a stationary random variable

$$F(s) \equiv B[t(s)]/B_{\text{ref}}[t(s)]. \tag{20}$$

The obvious choice for B_{ref} would be $B'(t)$, the root-mean-square value. This, however, is not available so, on grounds suggested in the next paragraph, we use the r.m.s. vorticity instead:

$$F \equiv [\omega_0'/\omega'(t)]\, B(t), \tag{21}$$

where $\omega_0' \equiv \omega'(t_0)$ is included so that F has the same dimensions as B. Each of the quantities in (21) is a component, but subscripts are omitted for simplicity. A prime denotes a root-mean-square value.

Recall (*a*) that the vorticity $\boldsymbol{\omega} \equiv \nabla \times \mathbf{u}$ is just twice the angular velocity of a *volume* element of fluid, (*b*) that a line element is rotated by both the vorticity and the strain rate, and (*c*) that the mean-square vorticity and strain rate are equal in isotropic turbulence. Therefore we *guess* that $\overline{B^2} \approx \overline{\omega^2}$.

† For velocity rescaling the r.m.s. turbulent velocity and the integral length scale are combined into a characteristic 'local' time scale (Townsend 1951, 1954; Comte-Bellot & Corrsin 1971).

Only slightly less obvious would be the choice of $[B'(t)]^{-1}$ as the local time scale, but again we use the r.m.s. component vorticity:

$$ds \equiv (\omega'(t)/\omega'_0)\,dt. \tag{22}$$

Equation (4) is applicable to decaying turbulence like that in the experiment, and we substitute (21) and (22) into it. The outcome is (omitting subscripts)

$$\frac{1}{2}\frac{d\overline{\Theta^2}}{ds} = \overline{\omega_0^2}\int_0^{s-s_0} L_F(\sigma)\,d\sigma, \tag{23}$$

where

$$L_F(\sigma) \equiv \overline{F(s)\,F(s\pm\sigma)}/\omega_0^2. \tag{24}$$

As $s-s_0 \to \infty$,

$$\frac{1}{2}\frac{d\overline{\Theta^2}}{ds} \to \overline{\omega_0^2}\,T_F. \tag{25}$$

The next step is to estimate $s(t)$ from (22).

Since the turbulence is approximately isotropic, we can estimate the vorticity from one of Taylor's forms for the energy decay rate (see, for example, Batchelor 1953):

$$d(\tfrac{1}{2}\overline{u_k u_k})/dt = -\nu\overline{\omega_i\omega_i}, \tag{26}$$

where ν is the kinematic viscosity. In the experiment time is, of course, proportional to downstream distance from the grid: $x_1 = \overline{U}t$.

Assuming that the mean-square velocity components decay approximately as in the straight-duct experiments summarized by Comte-Bellot & Corrsin (1966), we arrive at the estimate for a vorticity component:

$$\overline{\omega^2} \approx \frac{\overline{U}^2}{64\nu M}\left(\frac{\overline{U}t}{M}-2{\cdot}0\right)^{-2{\cdot}25}. \tag{27}$$

Then (22) becomes

$$ds = (\overline{U}t_0/M-2{\cdot}0)^{1{\cdot}125}\frac{dt}{(\overline{U}t/M-2{\cdot}0)^{1{\cdot}125}}. \tag{28}$$

When integrated from s_0 to s and from t_0 to t, this gives the rescaled time difference as

$$s-s_0 = \frac{8M}{\overline{U}}\left(\frac{\overline{U}t_0}{M}-2{\cdot}0\right)^{1{\cdot}125}\left\{\left(\frac{\overline{U}t_0}{M}-2{\cdot}0\right)^{0{\cdot}125}-\left(\frac{\overline{U}t}{M}-2{\cdot}0\right)^{-0{\cdot}125}\right\}. \tag{29}$$

For this particular experiment, $\overline{U} = 10{\cdot}16$ cm/s, $M = 1{\cdot}27$ cm and $\overline{U}t_0/M = 18$, so

$$\overline{U}(s-s_0)/M = 181\{0{\cdot}707-(8{\cdot}0t-2{\cdot}0)^{-0{\cdot}125}\}, \tag{30}$$

whose values are given in the second column of table 1.

Figure 2 presents the r.m.s. angular displacement as functions of 'corrected' time. According to (13) we can estimate the r.m.s. angular velocity at

$$\overline{U}t_0/M = 18 = \overline{U}s_0/M$$

by estimating the initial slope of the latter curve. The result (sketched) is

$$B'(t_0) = F'(s_0) = 1{\cdot}24\,\mathrm{s}^{-1}.$$

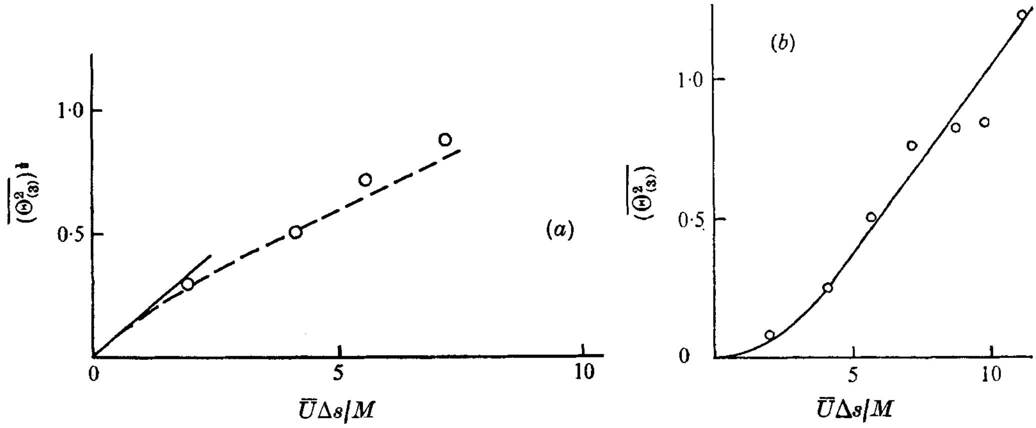

FIGURE 2. Angular displacement data 'corrected' for vorticity decay. (a) Root-mean-square value. (b) Mean-square value.

It is interesting to compare this with the 'measured' r.m.s. component vorticity estimated via (26): $\omega_0' \approx 1{\cdot}95\,\mathrm{s}^{-1}$, which is certainly the same order of magnitude, as conjectured.

Next, (16) can be invoked to estimate the integral time scale T_F from the roughly estimated (and sketched) asymptotic slope of the $\overline{\Theta^2}$ data. The result is

$$T_F \approx 0{\cdot}37\,\mathrm{s}.$$

We might wonder if the integral time scale of the angular velocity is comparable to the simplest characteristic time in the turbulence, viz. $(\omega')^{-1}$. In fact, this is so: $(\omega_0')^{-1} \approx 0{\cdot}51\,\mathrm{s}$.

Unfortunately there are too few data points to enable us to estimate the 'microscale' λ_F by applying (13).

5. The angular velocity in spatial co-ordinates

Any attempt to relate the angular dispersion to more accessible turbulence information, experimental or theoretical, must look at the expression for the angular dispersion in spatial ('Eulerian') co-ordinates. We are faced at once with the fact that the line element unit vector $\mathbf{l}$ obeys a complicated differential equation, and that equations for the angular displacements are even worse.

By techniques somewhat like those used by Batchelor (1952) to deduce the equation for time rate of increase of line element length, we can deduce that

$$\frac{D\mathbf{l}}{Dt} = l_i\frac{\partial \mathbf{u}}{\partial x_i} - \mathbf{l}l_j l_k\frac{\partial u_j}{\partial x_k}, \tag{31}$$

where $\mathbf{l}$ is the appropriate unit vector, the array of direction cosines, $\mathbf{u}(\mathbf{x},t)$ is velocity in a spatial frame, $\mathbf{x}$ is the spatial co-ordinate vector, t is time and $D/Dt \equiv \partial/\partial t + (\mathbf{u}\,.\,\nabla)$, the 'material time derivative', i.e. the spatial-frame expression for the time partial derivative in a material ('Lagrangian') frame. Equation (31) can also be written as

$$Dl_i/Dt = \tfrac{1}{2}l_j\omega_{ij} + \tfrac{1}{2}(\delta_{im} - l_i l_m)\,l_k e_{mk}\,, \tag{32}$$

where $\omega_{ij} \equiv \partial u_i/\partial x_j - \partial u_j/\partial x_i$ and $e_{ij} \equiv \partial u_i/\partial x_j + \partial u_j/\partial x_i$

are vorticity and strain-rate tensors.

Figure 1 (*b*) shows the three projected angles which would be measured by photographs along the Cartesian axes:

$$\theta_{(1)} = \tan^{-1}\left(\frac{l_3}{l_2}\right), \quad \theta_{(2)} = \tan^{-1}\left(\frac{l_1}{l_3}\right), \quad \theta_{(3)} = \tan^{-1}\left(\frac{l_2}{l_1}\right). \tag{33}$$

These, incidentally, satisfy

$$(\tan\theta_{(1)})(\tan\theta_{(2)})(\tan\theta_{(3)}) = 1. \tag{34}$$

From (33) we can deduce equations, expressed solely in terms of the $\theta_{(i)}$ and velocity gradients, for the time rates of increase of these three angles for a material line element:

$$\begin{aligned}\frac{D\theta_{(1)}}{Dt} = \cos^2\theta_{(1)}\Big\{&\cot\theta_{(3)}\frac{\partial u_3}{\partial x_1} + \frac{\partial u_3}{\partial x_2} + \tan\theta_{(1)}\frac{\partial u_3}{\partial x_3} \\ &-\tan\theta_{(1)}\left[\cot\theta_{(3)}\frac{\partial u_2}{\partial x_1} + \frac{\partial u_2}{\partial x_2} + \tan\theta_{(1)}\frac{\partial u_2}{\partial x_3}\right]\Big\},\end{aligned} \tag{35}$$

equations for $D\theta_{(2)}/Dt$ and $D\theta_{(3)}/Dt$ being given by cyclic permutation of all subscripts.

For particular line element orientations (which might be specified at t_0, the start of the dispersion process) these equations simplify considerably. We look at three simple cases.

$$\text{(i)} \quad \theta_{(1)} = \theta_{(2)} = \theta_{(3)} = \tfrac{1}{4}\pi. \tag{36}$$

Equation (35) here reduces to

$$\frac{D\theta_{(1)}}{Dt} = \frac{1}{2}\left\{\left(\frac{\partial u_3}{\partial x_1} + \frac{\partial u_3}{\partial x_2} + \frac{\partial u_3}{\partial x_3}\right) - \left(\frac{\partial u_2}{\partial x_1} + \frac{\partial u_2}{\partial x_2} + \frac{\partial u_2}{\partial x_3}\right)\right\}, \tag{37}$$

with similar expressions for $D\theta_{(2)}/Dt$ and $D\theta_{(3)}/Dt$.

$$\text{(ii)} \quad \theta_{(2)} = \theta_{(3)} = 0, \quad \theta_{(1)} \text{ undefined.} \tag{38}$$

(The direction cosines in this case are $l_1 = 1, l_2 = l_3 = 0$.) Here, (35) does not exist, but the other two equations become simply

$$\frac{D\theta_{(2)}}{Dt} = -\frac{\partial u_3}{\partial x_1}, \quad \frac{D\theta_{(3)}}{Dt} = \frac{\partial u_2}{\partial x_1}. \tag{39}$$

$$\text{(iii)} \quad \theta_{(1)} = \tfrac{1}{6}\pi, \quad \theta_{(2)} = \tfrac{1}{3}\pi, \quad \theta_{(3)} = \tfrac{1}{4}\pi. \tag{40}$$

In this case,

$$\frac{D\theta_{(1)}}{Dt} = \frac{3}{4}\left\{\left(\frac{\partial u_3}{\partial x_1} + \frac{\partial u_3}{\partial x_2} + \frac{1}{\sqrt{3}}\frac{\partial u_3}{\partial x_3}\right) - \left(\frac{1}{\sqrt{3}}\frac{\partial u_2}{\partial x_1} + \frac{1}{\sqrt{3}}\frac{\partial u_2}{\partial x_2} + \frac{1}{3}\frac{\partial u_2}{\partial x_3}\right)\right\}, \tag{41}$$

$$\frac{D\theta_{(2)}}{Dt} = \frac{1}{4}\left\{\left(\sqrt{3}\frac{\partial u_1}{\partial x_2} + \frac{\partial u_1}{\partial x_3} + \sqrt{3}\frac{\partial u_1}{\partial x_1}\right) - \left(3\frac{\partial u_3}{\partial x_2} + \sqrt{3}\frac{\partial u_3}{\partial x_3} + 3\frac{\partial u_3}{\partial x_1}\right)\right\}, \tag{42}$$

$$\frac{D\theta_{(3)}}{Dt} = \frac{1}{3}\left\{\left(\frac{1}{\sqrt{3}}\frac{\partial u_2}{\partial x_3} + \frac{\partial u_2}{\partial x_1} + \frac{\partial u_2}{\partial x_2}\right) - \left(\frac{1}{\sqrt{3}}\frac{\partial u_1}{\partial x_3} + \frac{\partial u_1}{\partial x_1} + \frac{\partial u_1}{\partial x_2}\right)\right\}. \tag{43}$$

For *isotropic turbulence* these 'initial' angular velocity components have roughly equal mean-square values.

$$\text{Case (i)}\quad \overline{\left(\frac{D\theta_{(1)}}{Dt}\right)^2} = \overline{\left(\frac{D\theta_{(2)}}{Dt}\right)^2} = \overline{\left(\frac{D\theta_{(3)}}{Dt}\right)^2} = 2f_0''\overline{u^2}, \tag{44}$$

where $f(r)$ is the Kármán–Howarth 'longitudinal' correlation coefficient function of velocity, the primes denote derivatives and $\overline{u^2}$ is the mean-square *component* velocity.

$$\text{Case (ii)}\quad \overline{\left(\frac{D\theta_{(2)}}{Dt}\right)^2} = \overline{\left(\frac{D\theta_{(3)}}{Dt}\right)^2} = 2f_0''\overline{u^2}. \tag{45}$$

$$\text{Case (iii)}\quad \left.\begin{aligned} \overline{\left(\frac{D\theta_{(1)}}{Dt}\right)^2} = \overline{\left(\frac{D\theta_{(2)}}{Dt}\right)^2} &= \tfrac{7}{2}f_0''\overline{u^2}, \\ \overline{\left(\frac{D\theta_{(3)}}{Dt}\right)^2} &= \tfrac{28}{27}f_0''\overline{u^2}. \end{aligned}\right\} \tag{46}$$

It is interesting that these components are all of the same order of magnitude. To compute the mean-square angular velocity of an arbitrarily oriented line element we would have to square (35), for example, and integrate it with the weightings of $\theta_{(1)}$, $\theta_{(2)}$ and $\theta_{(3)}$ appropriate to isotropic initial line orientation.

As a magnitude comparison with the values in (44), (45) and (46), we recall that the mean-square value of a Cartesian component of *vorticity* in isotropic turbulence is $5f_0''\overline{u^2}$.

6. The approach of a scalar field toward isotropy

Angular dispersion is a possible framework within which to consider the approach toward isotropy of an initially anisotropic scalar field being mixed by an isotropic turbulence. Such an initial-value problem, though an obvious prelude to the more difficult one of how turbulence itself tends to become isotropic, seems to have been ignored in the scientific literature. The only work known to us is an unpublished report by O'Brien (1963).

To illustrate the question, consider a scalar field initially consisting of isotropically positioned, short straight lines all parallel, see figure 3(*a*). If all the lines are much shorter than the Kolmogorov microscale of the isotropic turbulence which convects them, and if there is no molecular diffusion, the scalar field will presumably become very nearly isotropic by the time the root-mean-square angular dispersion is much larger than $\frac{1}{2}\pi$:

$$\Theta'_{(i)} \gg \tfrac{1}{2}\pi. \tag{47}$$

Figure 3(*b*) is a qualitative sketch of a single realization.

The isotropic state is, of course, not uniquely prescribed by the Θ's of the marked line elements. It is established rather by their probability density over the interval

$$n\pi \leqslant \Theta_{(t)} \leqslant (n+1)\pi, \tag{48}$$

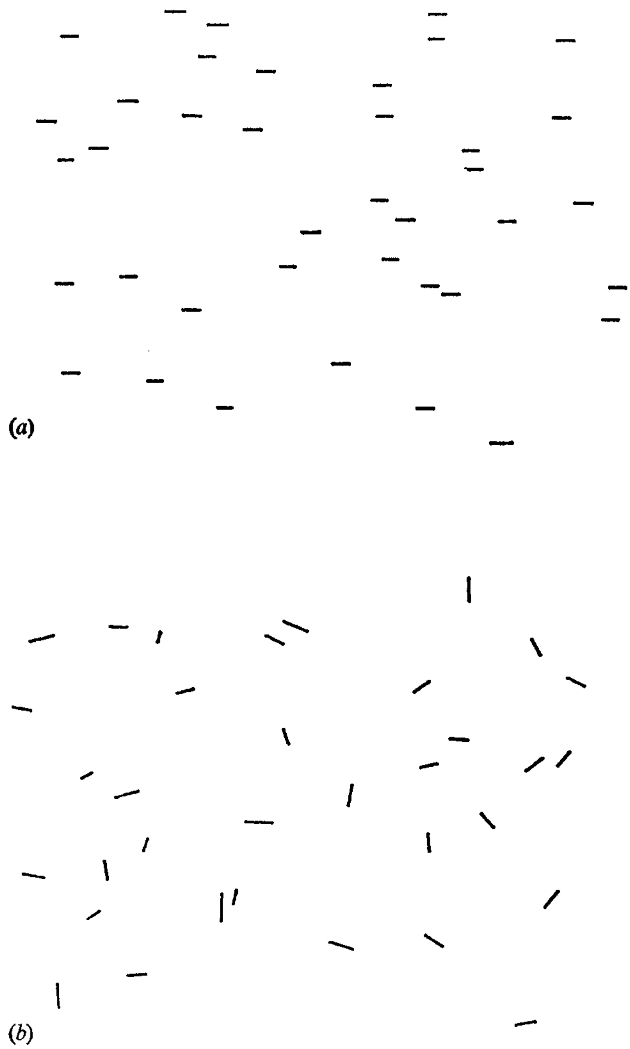

FIGURE 3. Qualitative sketch of the angular dispersion of a single realization of material line elements. (*a*) Start, $t = t_0$. (*b*) Virtually isotropic.

where all integer values of n are included. In other words, in figure 3(*b*) it is the actual *observed* orientation angle α (say) in the range $0 \leqslant \alpha \leqslant \pi$ which decides the isotropy, independently of the value of n in the equation

$$\alpha = \Theta - n\pi. \tag{49}$$

In order to get a rough idea of the degee of the inequality in (47) needed for any specific departure from isotropy, it is instructive to suppose that Θ is Gaussian, and to look at the probability density function of α for various ratios $\Theta'/(\frac{1}{2}\pi)$. Figure 4 shows p_α, the probability density function of α, plotted radially on the outside of a circle for three different (rather small) values of Θ'. In effect we have simply wrapped the Gaussian function around the circle, summing the overlapping parts. The relatively small value of Θ' corresponding to effective

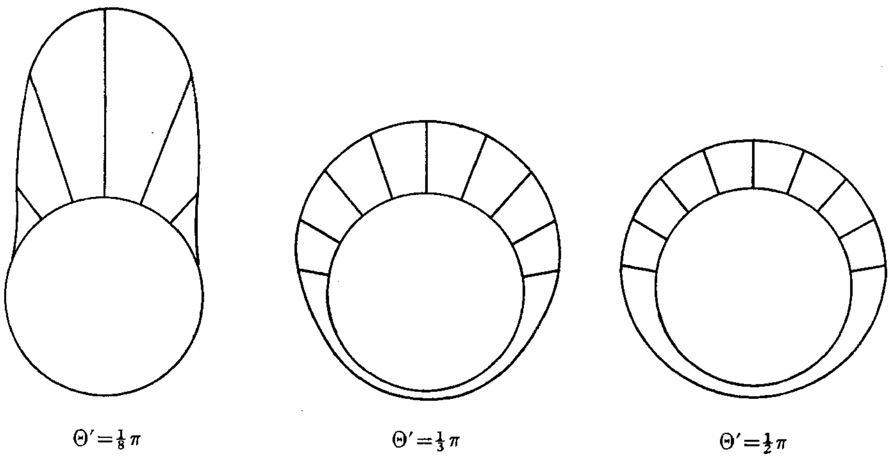

FIGURE 4. Normal ('Gaussian') probability density function of angle, wrapped around a circular base.

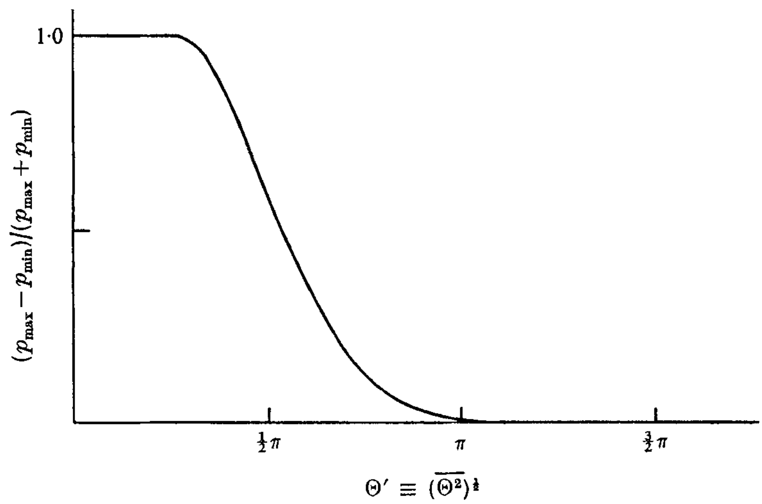

FIGURE 5. Degree of isotropy as a function of r.m.s. angular displacement.

isotropy is illustrated by figure 5, which gives a direct measure of the lopsidedness of p_α. By the time $\Theta' = \pi$, the field is essentially isotropic. This suggests that (47) is much too strong a condition.

If the initial scalar field were an array of infinite parallel lines, it is clear that both translational dispersion and angular dispersion would play a role in the approach toward isotropy.

This work was supported by the Fluid Dynamics Branch, U.S. Office of Naval Research, and was presented in November 1967 at the Annual Meeting of the Division of Fluid Dynamics, American Physical Society. We should like to thank D. J. Shlien for help in reducing the data, and to acknowledge the encouragement of the Society for Statistical Geometry.

REFERENCES

BATCHELOR, G. K. 1952 *Proc. Roy. Soc.* A **213**, 349.

BATCHELOR, G. K. 1953 *The Theory of Homogeneous Turbulence*, p. 86. Cambridge University Press.

BATCHELOR, G. K. & TOWNSEND, A. A. 1956 In *Surveys in Mechanics* (ed. G. K. Batchelor & R. M. Davies). Cambridge University Press.

COMTE-BELLOT, G. & CORRSIN, S. 1966 *J. Fluid Mech.* **25**, 657.

COMTE-BELLOT, G. & CORRSIN, S. 1971 *J. Fluid Mech.* **48**, 273.

CORRSIN, S. 1962 In *Mécanique de la Turbulence*. Paris: C.N.R.S.

CORRSIN, S. & KARWEIT, M. J. 1969 *J. Fluid Mech.* **39**, 87.

KARWEIT, M. J. 1968 M.S.E. thesis, The Johns Hopkins University.

LUMLEY, J. L. 1962 In *Mécanique de la Turbulence*. Paris: C.N.R.S.

LUMLEY, J. L. 1970 *Stochastic Tools in Turbulence*, §3.9. Academic.

O'BRIEN, E. E. 1963 On the behaviour of passive scalars in a turbulent fluid. *State University of New York, Stony Brook Rep.*

TAYLOR, G. I. 1921 *Proc. Lond. Math. Soc.* **20**, 196.

TOWNSEND, A. A. 1951 *Proc. Roy. Soc.* A **209**, 418.

TOWNSEND, A. A. 1954 *Proc. Roy. Soc.* A **224**, 487.